Low temperature electrical transport in ferromagnetic Ni nanowires

M. Venkata Kamalakar* and A. K. Raychaudhuri†
Department of Material Sciences, DST Unit for NanoSciences, S. N. Bose National Centre for Basic Sciences, Block JD, Sector III, Salt Lake, Kolkata 700 098, West Bengal, India
(Received 27 December 2008; published 19 May 2009)

We report the electrical transport properties of arrays of nickel nanowires (diameters ranging from 55 to 13 nm) fabricated by electrodeposition into the cylindrical pores of anodic alumina membranes. X-ray and transmission electron microscope based characterization ensured single crystalline nature of the nanowires. We have measured the resistance of the nickel nanowires in the temperature range of 3–300 K with the specific aim of probing the effect of size reduction on the temperature dependence of resistivity. As the lateral dimension decreases, deviations from the bulk resistivity are observed. Our work reveals intrinsic differences in the transport mechanisms taking place in these wires when the diameter of the wires is brought down from bulk to nano regime. The resistance data has been analyzed using the Bloch-Wilson function and the Debye temperature (θ_R) was calculated from the fits. The Debye temperature showed a systematic decrease with decrease in diameter, which we note is a trend in other fcc metals such as Ag and Cu. We observed an increase in the residual resistivity as the diameter decreases due to surface scattering. We further observe a strong suppression in the spin wave contribution to the resistivity of the magnetic nanowires as the diameter is decreased. We discuss the likely causes for these changes.

DOI: 10.1103/PhysRevB.79.205417 PACS number(s): 73.63.−b, 72.15.−v

I. INTRODUCTION

Research on nanostructures has led to the exploration of novel physics and material properties at reduced physical dimensions. The influence of reduced physical dimensions is of both fundamental and technological interest. Nanoscale arrays of magnetic materials have large potential in wide range of applications including magnetic data storage, nanoelectromechanical systems, sensors and actuators, nanoscale spintronic devices, etc. Magnetic nanowires represent an important variety of magnetic nanostructures. The resistance of a magnetic nanowire becomes a subject matter of immense interest when applications such as electronic and spintronic devices are concerned. While a lot of work has been done on the magnetic properties of nickel nanowires,[1–3] the electrical transport properties remain vastly unexplored. In the regime where the diameter of the nanowires is few tens of nanometers and the carrier mean free path is limited by the wire dimensions, the resistivity depends not only on the material but also on its size.[4–8] Although the transport becomes that of quantum nature when the diameter of nanowire gets closer to the molecular size, there is a considerable size range (few tens of nanometers in case of metals) where the Boltzmann transport theory is applicable,[9] yet it is modified by finite-size effects. This typically occurs in metallic nanowires with diameter <100 nm. Interestingly, this is also the diameter regime where technical applications are envisaged.

In this paper we present a detailed study of the electron transport in single crystalline nanowires of various diameters (55, 35, 18, and 13 nm). There are three essential points which this paper attempts to address: (a) what happens to the electron-phonon interaction and whether a single Debye-temperature description can explain the data, (b) the effect of surface scattering on the residual resistivity, and (c) what happens to the electron-magnon interaction as the diameter of the nanowire is reduced. In this work, we measured the resistance of oriented single crystalline nickel nanowires in the temperature range of 3–300 K. The wires are ferromagnetic with T_C above room temperature. The resistance of a pure nickel bulk wire (~ 50 μm) is also measured as a reference. We note that developing a scheme where temperature dependence of resistivities of nanowires with diameters of 10 nm or above can be estimated is a fruitful exercise because it gives a predictive test that resistivities can be estimated without actually measuring it in every sample. We also show that the experiment gives us a way to determine the Debye temperature (θ_R) for the nanowires and gives us a way to predict what happens to the elastic modulus on size reduction. The results obtained also show that the magnetic contribution to resistivity is severely suppressed on size reduction.

II. RESISTIVITY OF A 3*d* FERROMAGNETIC METAL

For simple nonmagnetic metals such as Cu, Ag, and Au, the resistivity ρ is composed of a temperature independent residual resistivity ρ_0, which arises from the scattering of electrons from lattice defects and impurities, and a temperature dependent lattice contribution ρ_L, which originates from the scattering of conduction electrons by lattice phonons,[10]

$$\rho = \rho_0 + \rho_L. \tag{1}$$

The temperature dependent part of electrical resistivity ρ_L is well described by the Bloch-Grüneisen (BG) function, $f(\frac{T}{\theta_R})$,

$$\rho_L = \alpha_{\text{el-ph}} f(T/\theta_R), \tag{2}$$

$$f\left(\frac{T}{\theta_R}\right) = \left(\frac{T}{\theta_R}\right)^n \int_0^{(\theta_R/T)} \frac{x^n dx}{(e^x - 1)(1 - e^{-x})}, \tag{3}$$

where θ_R is the Debye temperature as observed from resistivity. In most cases it closely matches with θ_D as obtained from other methods such as heat capacity measurement.

Generally, $n=5$ for simple metals and alloys. $\alpha_{\text{el-ph}}$ is a constant that is $\propto \lambda_{\text{tr}}\omega_D/\omega_p^2$, where λ_{tr} is the electron-phonon coupling constant, ω_D is the Debye frequency, and ω_p is the plasma frequency. It has been shown by our group before that in nonmagnetic metallic nanowires such as Cu or Ag, the temperature dependent resistivity can be quantitatively described by the BG formula[9] even for wires with diameter as low as 15 nm. In case of magnetic materials, in addition to electron-phonon interactions, other mechanisms of scattering exist which can give rise to additional contribution to the temperature dependence of ρ. Unlike simple metals, the electrical resistivity of 3*d* ferromagnetic transition metals such as Ni, Co, and Fe have a magnetic contribution ρ_M as the electrons get scattered by magnons at low temperatures. It is of interest to check what happens to the magnetic contribution, ρ_M, when the size is reduced below 100 nm. The total resistivity (ρ) is the sum of the contributions (Matthiessen's rule) due to potential scattering (ρ_0), phonon scattering (ρ_L), and magnetic scattering (ρ_M),

$$\rho = \rho_0 + \rho_L + \rho_M. \tag{4}$$

In case of a ferromagnetic metal the *s* and *d* bands overlap at the Fermi level. So for both lattice and magnetic scattering, conduction electrons might undergo *s*-*s* (intraband) as well as *s*-*d* (interband) transitions. Typically, for magnetic metals and alloys with large *d*-band density of states giving rise to electron-phonon scattering involving *s*-*d* transitions, the scattering of conduction electrons by phonons is described by the Bloch-Wilson formula[11] with $n=3$ in Eqs. (1)–(3). The magnetic scattering arises from the exchange interaction between the conduction electrons and the more localized magnetic electrons (3*d*), commonly called *s*-*d* interaction. Using a spin wave description, Mannari[12] found the following expression for ρ_M:

$$\rho_M = BT^2; \quad B = \frac{3\pi^5 S\hbar}{16e^2k_F}\left(\frac{\mu}{m}\right)^2\frac{[k_BTNJ(0)]^2}{E_F^4}, \tag{5}$$

where S (=1/2) is spin of the conduction electron, μ is the effective magnon mass, and m is the electron mass. For Ni, the ratio $\mu/m \approx 38$, E_F is the Fermi energy, k_F = Fermi wave vector, and $NJ(0)$ is the strength of the *s*-*d* interaction in the long wavelength limit (≈ 0.48 eV for Ni), N being the number of spins. For Ni, the above relation gives $B \approx 1.1\times10^{-13}$ Ω m K^{-2} which matches very well with that obtained experimentally in bulk Ni.

In the bulk 3*d* transition metals and alloys, a $\rho_M \propto T^2$ (considering the *s*-*s* electron-magnon scattering) behavior for $T < 15$ K has been reported.[12,13] At temperatures $T > 15$ K, there are additional terms and the scattering process has a complicated temperature dependence.

In this paper, we have investigated the effect of size reduction on the magnetic term in the electrical resistivity in case of nickel nanowires. Our analysis shows how the resistivity (ρ) changes as we decrease the diameter of the nanowires where the electron mean free path becomes comparable to the diameter of the nanowires. [Note: in this investigation, our analysis is limited to the upper temperature range of 300 K only. For $T > 300$ K as $T \rightarrow T_C$ (ferromagnetic Curie point), the spin disorder and critical scattering become important.]

III. EXPERIMENTAL

The nickel nanowire arrays with diameters in the range of 55–13 nm were prepared using a pulsed potentiostatic electrodeposition technique using commercially available standard anodic alumina templates.[14] The pore diameters of the templates were checked using scanning electron microscopy (SEM). The templates have a thickness of 50–60 μm. A layer of 200 nm of silver is evaporated on to one surface of the nanoporous templates in a thermal evaporation chamber. The coated side of the template was used as the working electrode with the uncoated surface facing the electrolyte in a three electrode potentiostatic deposition bath. Saturated calomel electrode (SCE) and platinum electrode are the reference and the counter electrodes respectively. The depositions were carried out with a 300 g/l $NiSO_4\cdot6H_2O$, 45 g/l $NiCl_2\cdot6H_2O$, and 45 g/l H_3BO_3 solution as the electrolyte with the working electrode at a pulse potential of -1 V with respect to the SCE with 80% duty cycle and pulse period of 1 s. Electrodeposition continued until the nickel filled the pores and came out to the side exposed to the electrolyte as observed by an increase in the current. The extra layer of nickel deposited on the template side facing the electrolyte was removed by polishing. The wires thus prepared were characterized using x-ray diffraction (XRD), transmission electron microscopy (TEM), and SEM. Powder x-ray diffraction using Cu $K\alpha$ radiation was carried out by retaining the wires inside the alumina templates. For scanning electron microscopy, the template was partially etched out by keeping them immersed in 3M NaOH solution for about 10 min and then washing out the dissolved parts with distilled water. For transmission electron microscopy, the templates were etched out completely by keeping them immersed in 6M NaOH solution for about 30 min. The nanowires in the templates were annealed at 600 K in 10^{-6} mbar vacuum. The resistance of the wires was measured in the temperature range of 3–300 K using pseudo four probe method[9] in a pulsed tube based closed cycle refrigerator[15] using a low frequency (174.73 Hz) ac current of 100 μA with a resolution of 10 ppm.

IV. RESULTS

A. Structural characterization

The structural and crystallographic nature of the wires constitute an important part in the analysis of the data. The wires used in this investigation are single crystalline and oriented in nature. This has been established by techniques such as XRD and high resolution transmission electron microscopy. The structural data have been shown in Fig. 1. The data shown in Fig. 1 is for a 55 nm diameter wire and it is typical for other wires as well. The x-ray diffraction pattern shown in Fig. 1(a) reveals that the nanowires grown have a preferential direction [(220)] of growth. Figure 1(b) shows a transmission electron micrograph of a 55 nm diameter nano-

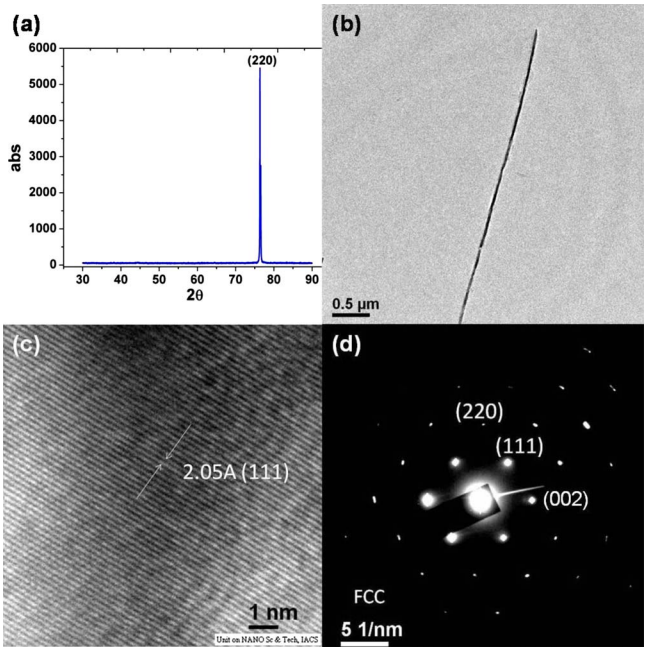

FIG. 1. (Color online) (a) XRD pattern of 55 nm diameter nanowire arrays, (b) TEM image of a 55 nm diameter nanowire, (c) HRTEM image of the lattice planes in a 55 nm diameter nanowire, and (d) the electron diffraction pattern of a 55 nm diameter nanowire.

wire. A high resolution transmission electron micrograph (HRTEM) is shown in Fig. 1(c). The electron diffraction pattern shown in Fig. 1(d) confirms that the nanowires are single crystalline and confirms the fcc nature of the crystal structure. The fact that the wires are single crystalline is very important because this ensures that the residual resistivity (ρ_0) comes predominantly from the surface scattering of electrons in absence of scattering at any grain boundary. As a check on the lattice parameter the value of lattice constant obtained from the XRD data is ~3.55 Å for different nanowires.

B. Electrical transport

The electrical resistance measurements were carried out by retaining the wires within the alumina membrane. The resistance of the nanowire arrays is measured by pseudo four probe method in which two electrical leads were attached to each of the two sides of the membrane containing nanowires using silver epoxy. The method and the issues related to contact resistance and contact noise have been discussed in details in previous publications by the group.[9,16,17] In the case of 50 μm diameter bulk nickel wire, the resistance is measured by simple four probe method. The resistance data of nanowires (normalized by resistance at 300 K) along with the bulk nickel wire is shown in Fig. 2. Schematic representations of the four probe and pseudo four probe methods are shown in the corresponding insets [Figs. 2(a) and 2(b)] respectively. A first look into the plot shows that the wires become more resistive as the diameter decreases. We could successfully put four probes on a single nanowire of diameter 55 nm using focused ion beam, and the resistivity determined by the four probe method matches well with that determined by retaining them in the array in the template. Thus the contact resistance is not significant. We comment on this later on. In the following subsection we analyze the resistance data.

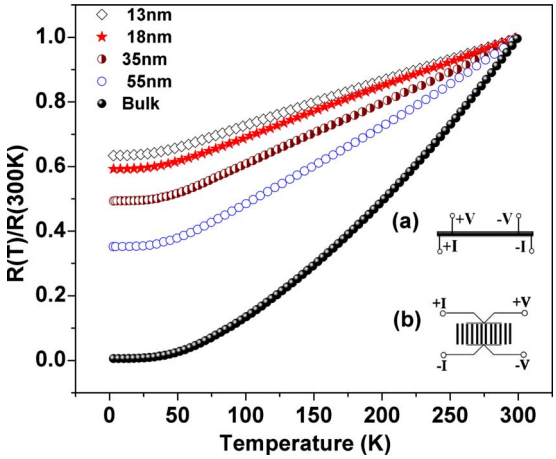

FIG. 2. (Color online) Normalized plot of resistance data of the nanowires as compared with the bulk wire; Schematic representations of (a) four probe method and (b) pseudo four probe configurations.

C. Analysis of electrical resistance data for $T > 15$ K

The first part of our analysis is to investigate the temperature dependence of the resistance R. The electrical resistivity of a $3d$ ferromagnetic material can be described by Eq. (4). At very low temperatures ($T < 15$ K), the magnetic part varies with temperature as $\rho_M = BT^2$. Beyond 15 K, the magnetic contribution has a complicated temperature dependence because of additional intraband s-d electron-magnon scattering. However, well below the Debye temperature and above 15 K, the main temperature dependent term that dominates the resistivity is the electron-phonon interaction term (ρ_L). We explore whether the temperature dependence of the resistance can be explained in the frame work of the Boltzmann transport theory using Eqs. (1)–(3). As discussed, ρ_M for $T > 15$ K is generally much less than ρ_L. We thus fit the resistance data for 15 K $\leq T \leq$ 100 K using Eq. (6). The best fit is obtained with $n=3$ (Bloch-Wilson formula),

$$R = R_0 + \alpha\left(\frac{T}{\theta_R}\right)^n \int_0^{\theta_R/t} \frac{x^n dx}{(e^x - 1)(1 - e^{-x})}, \qquad (6)$$

α is related to $\alpha_{\text{el-ph}}$ [Eqs. (1)–(3)] by the same geometric factor that relates R to ρ. The analysis as in Eq. (6) using R instead of ρ allows us to explore the temperature dependence and determine θ_R without the uncertainty in the absolute value of ρ. The fit parameters R_0, α, and θ_R were optimized to give a relative fit error (defined in percentage as $\frac{(R_{\text{measured}} - R_{\text{fit}})}{R_{\text{measured}}} \times 100$) of less than 0.4% over the entire range. A typical fit is shown in Fig. 3 for nanowires of diameter of 35 nm. The Debye temperature of 471 K for the bulk wire of 50 μm diameter as estimated from the fitting matches with

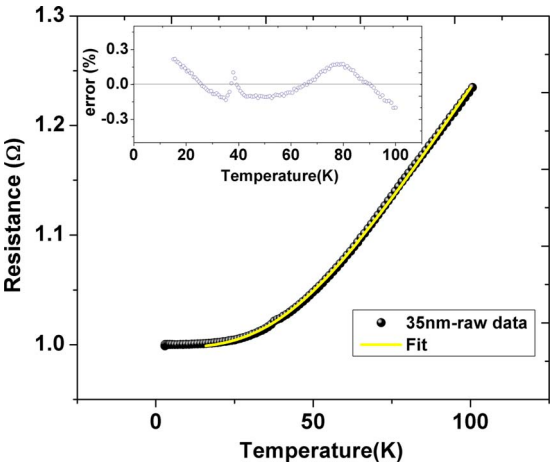

FIG. 3. (Color online) Resistance vs temperature data of a 35 nm diameter nanowire fit between 15–100 K. The inset shows the percentage fit error.

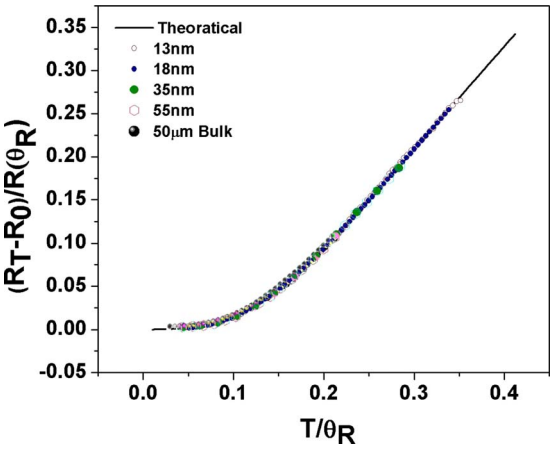

FIG. 4. (Color online) Plot of $\frac{R-R_0}{R(\theta_R)}$ as a function of $\frac{T}{\theta_R}$.

accepted value.[10] The values of Debye temperature obtained for wires of various diameters are tabulated in Table I. We will discuss the size dependence of θ_R in the Sec. V.

To check whether a single parameter description of ρ_L using θ_R is valid for the nanowires, we used the following procedure. From Eqs. (1)–(3), we obtain the following relation:

$$\rho_L(T) = \rho - \rho_0, \tag{7}$$

$$\frac{\rho_L(T)}{\rho(\theta_R)} = \frac{\rho - \rho_0}{\rho(\theta_R)}$$

$$= \frac{R - R_0}{R(\theta_R)}. \tag{8}$$

This shows that if the BG equation is valid, then $\frac{\rho-\rho_0}{\rho(\theta_R)}$ and hence, $\frac{R-R_0}{R(\theta_R)}$ is a unique function of $\frac{T}{\theta_R}$. $R(\theta_R)$ and $\rho(\theta_R)$ are the values of the phonon contribution to the resistance and the resistivity respectively evaluated at Debye temperature θ_R. If indeed the ratio in Eq. (8) is a unique function of $\frac{T}{\theta_R}$, then for all the nanowires the resistance curves can be scaled into a single curve provided that all of them have the same electron-phonon coupling constant $\alpha_{\text{el-ph}}$. In Fig. 4, we plot the data for all the nanowires ($\frac{\rho-\rho_0}{\rho(\theta_R)}$ vs $\frac{T}{\theta_R}$). It can be seen that the data for all the wires collapse into a single curve. This ensures that a single parameter description using θ_R is valid. This also confirms that $\alpha_{\text{el-ph}}$ is independent of the wire diameter.[9] This is an important observation and it allows us to estimate the absolute value of resistivity of nanowires as explained below.

D. Absolute value of resistivity

Determination of the absolute value of the resistivity (ρ) of the nanowire from the observed resistance R of the array is not a straight forward issue because of the uncertainty in the determination of the number of wires in the array. A method has been used by our group[9] to determine the value of ρ that does not need counting of the number of wires. We use this method here, and more importantly also validate the method by measurement of the resistivity of a single nanowire of a given diameter. The method is a general method and uses the fact that the temperature dependence of the resistivity at $T < \theta_R$ is determined by the electron-phonon contribution only. For nanowires of nonmagnetic materials (where electron-phonon interaction is the only cause of temperature dependence), this can be successfully employed over the whole range of T. For magnetic nanowires this can also be used to a temperature up to which the contribution by magnetic scattering compared to the electron-phonon scattering is negligible. We extend the method to the case of magnetic nanowires and restrict our analysis to a moderate temperature of 100 K (to avoid any considerable contribution due to spin wave scattering of both *s-s* and *s-d* electron-magnon interactions which increase as the temperature is in-

TABLE I. Summary of the analyzed resistance data.

Wire diameter (nm)	$\rho_{4.2\ \text{K}}$ (Ω m)	$\rho_{300\ \text{K}}$ (Ω m)	θ_R (K)	B (Ω m K^{-2})
50000	0.022×10^{-8}	6.879×10^{-8}	471.209	$(1.529\pm0.072)\times10^{-13}$
55	3.853×10^{-8}	1.094×10^{-7}	350.828	$(1.397\pm0.092)\times10^{-13}$
35	6.537×10^{-8}	1.324×10^{-7}	342.280	$(9.728\pm0.423)\times10^{-14}$
18	1.679×10^{-7}	2.761×10^{-7}	296.839	$(6.128\pm0.457)\times10^{-14}$
13	1.793×10^{-7}	2.852×10^{-7}	283.678	$(4.751\pm0.091)\times10^{-14}$

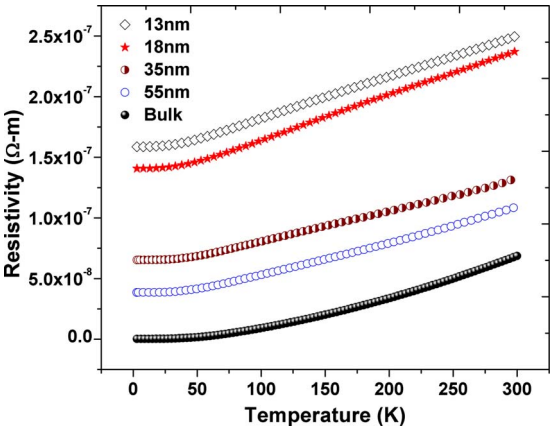

FIG. 5. (Color online) Resistivities of the nanowires as compared with the bulk wire.

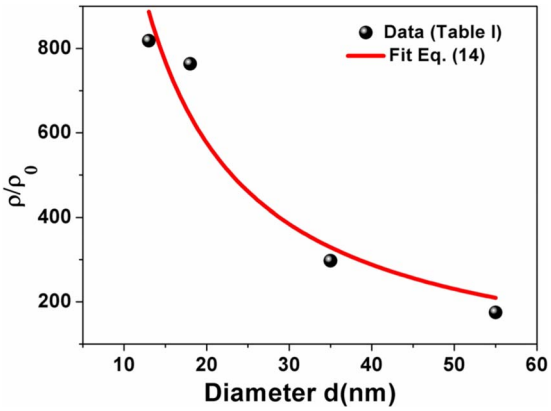

FIG. 6. (Color online) Fit of Eq. (14) to the resistivity data of the nanowires at $T = 4.2$ K.

creased), and preferred exact calculations instead of approximations which have been done earlier.[9]

In the temperature of interest (15–100 K), the predominant temperature dependent part of the resistivity in the magnetic nanowires arises from the electron-phonon interaction part [because Eq. (6) fits very well up to 100 K]. This can be further understood later from Fig. 9, where we observe a suppression in spin wave resistivity as the diameter of the wire is decreased. As a result we can use, for $T < 100$ K,

$$\frac{d\rho}{dT} = \frac{d\rho_L}{dT}, \tag{9}$$

$$\frac{d\rho}{dT} = \alpha_{\text{el-ph}} f^1, \tag{10}$$

where $f^1 = \frac{df}{dT}$. If ρ_B and ρ_N are the resistivities of the bulk and nanowire, respectively, at any given temperature, then

$$\frac{\frac{d\rho_N}{dT}}{\frac{d\rho_B}{dT}} = \frac{f_N^1}{f_B^1}, \tag{11}$$

$$\frac{\rho_N}{\rho_B}\frac{(\text{TCR})_N}{(\text{TCR})_B} = \frac{f_N^1}{f_B^1}, \tag{12}$$

$$\rho_N = \frac{f_N^1}{f_B^1}\frac{(\text{TCR})_B}{(\text{TCR})_N}\rho_B, \tag{13}$$

where $\text{TCR} = \frac{1}{\rho}\frac{d\rho}{dT} = \frac{1}{R}\frac{dR}{dT}$ is the temperature coefficient of resistivity, and the subscripts B and N refer to the bulk and nanowire respectively. Both these quantities are directly obtained from measurements. The $f^1(N)$ and $f^1(B)$ can be directly calculated since we know the values of the respective θ_R. Thus all the quantities on the right-hand side of Eq. (13) are known. In our case the resistivity of bulk nickel wire was 8.6×10^{-9} Ω m at 100 K. Using this value, the resistivity of nanowires were calculated in the temperature range of interest using Eq. (13). Figure 5 shows the resistivities of the nanowires evaluated. Although the resistivity of the nanowires is of the same order as reported earlier,[18] our samples are less resistive because of better crystallinity.

To validate the above procedure we made measurements on a single nanowire. We were able to connect four platinum probes (width ≈ 500 nm) along the length of a single Ni nanowire of diameter 55 nm by using focused ion beam. The wires were removed from the membrane by dissolving the membrane in NaOH and the wires were spread on insulating Si substrate. The resistivity values for the single nanowire at 4.2 K, 100 K, and 300 K are 4.12×10^{-8}, 5.2×10^{-8}, and 9.45×10^{-8} Ω m, respectively, and these values match closely (within a maximum error of 10%) with the values determined by the above procedure.

E. Resistivity at 4.2 K and surface scattering

The determination of the absolute value of the resistivity, and in particular, the absolute value at 4.2 K ($\rho_{4.2\ \text{K}}$) allows us to investigate the role of surface scattering in determination of the residual resistivity.

To understand the effect of surface scattering, we have fit $\rho_{4.2\ \text{K}}$ with the surface scattering model[19] for wires of diameter $d \ll l$ given as

$$\frac{\rho(d)_{4.2\ \text{K}}}{\rho_0} = \frac{1-p}{1+p}\frac{l}{d}, \tag{14}$$

where $\rho(d)_{4.2\ \text{K}}$ and ρ_0 are the resistivity of the nanowire of diameter d and that of the bulk metal, respectively, at 4.2 K, and l is the electron mean free path of the bulk wire. p is the specularity coefficient, which is the fraction of electrons getting elastically scattered from the wire boundary. The dependence of $\rho(d)_{4.2\ \text{K}}$ on d can be seen in Fig. 6. From the fit to Eq. (14) (shown in Fig. 6), we obtained $p = 0.05$. p has been assumed to be more or less the same for all the wires. The fit of the data to Eq. (14) validates this assumption. The value of p obtained by us is much less in comparison to that in noble metals.

Determination of the specular coefficient p allows us to find the mean free path of electrons (l_d) in a nanowire of diameter d at 4.2 K. The following relation,[20] valid for $d \ll l$, was used

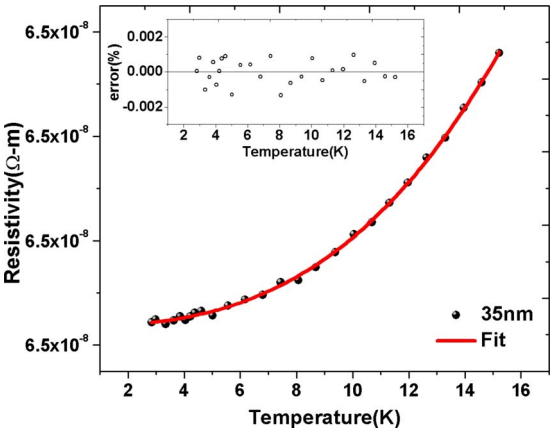

FIG. 7. (Color online) The low temperature resistivity data ($T < 15$ K) of 35 nm diameter nanowire being fit to Eq. (4). The inset shows the percentage fit error.

$$l_d = \frac{1+p}{1-p} d. \tag{15}$$

From Eq. (15), with $p = 0.05$, the electron mean free path in nanowires at 4.2 K comes out to be 1.1 times the diameter of the nanowires. This is an interesting result because the mean free path of the electrons in the nanowires is as large as the diameter of the wire. Since the wire diameter puts a limit to electron mean free path, the surface scattering is dominant. The low value of p implies that the surface scattering is diffused in nature. The above observation shows that the electrons do not suffer appreciable scattering within the volume of the nanowire since the nanowires are single crystalline.

F. Magnetic contribution to the resistivity

At very low temperatures ($T < 15$ K), the magnetic part varies with temperature as $\rho_M = BT^2$ in $3d$ ferromagnets as given in Eq. (5). The resistivity data for temperatures $T < 15$ K is analyzed using Eq. (4) to estimate the contribution due to magnetic scattering arising out of spin fluctuations. For the case of bulk nickel wire (50 μm), we found that the resistivity ρ indeed has a quadratic dependence on T and $B = 1.53 \times 10^{-13}$ Ω m K^{-2}, which is in excellent agreement with previous theoretical and experimental reports.[12,13] A typical fit of Eq. (4) is shown in Fig. 7 for the 35 nm diameter nanowires. The inset shows the fit percentage error, which is less than 0.001%. In Fig. 8 we show $\rho_M(T < 15$ K), the magnetic contribution to the resistivity, (obtained after removing the residual and the lattice parts of resistivity) of the nanowires below $T < 15$ K. Since below the mentioned temperature the magnetic contribution to the resistivity is mainly due to s-s electron-magnon kind which follows Eq. (5), we plot $\rho_M(T < 15$ K) as a function of T^2. For all the nanowires the T^2 dependence persists, and there is a systematic decrease in B as the diameter is reduced [Fig. 10(b)]. B is considerably lower for lowest diameter wires used in our study compared to that in the bulk. The values of B are tabulated in Table I.

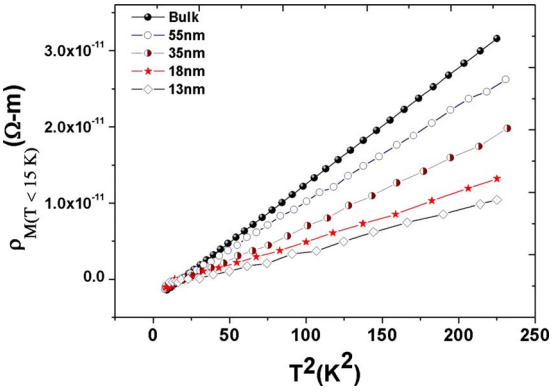

FIG. 8. (Color online) Plot of magnetic part of resistivity $\rho_M(T < 15$ K) versus T^2 for $T < 15$ K.

For temperatures $T > 15$ K and above, the magnetic contribution to the resistivity $\rho_M(T > 15$ K) is expected to show a complicated behavior due to both intraband (s-s) and interband (s-d) kinds of electron-magnon scattering.[21] To assess the contribution of the magnetic scattering, in Fig. 9 we show the $\rho_M(T > 15$ K), which is obtained from the observed resistivity after removing the residual resistivity and the lattice part of resistivity. This is plotted as a function of T. In this case also we see a suppression of magnetic contribution over the complete temperature range as the wire diameter is lowered. In the bulk wire there is sufficient contribution of magnetic scattering for $T > 100$ K. In nanowires it is much less compared to the temperature dependent lattice part of the resistivity (ρ_L).

V. DISCUSSIONS

In analyzing our data, we took $T = 15$ K as the optimum temperature below which we analyzed the s-s electron-magnon scattering's T^2 dependence and above which we analyzed the resistance with the Bloch-Wilson[11] model. This is because of two main reasons. First, it has been established theoretically[12,22,23] that the temperature dependent part is mainly dominated by the s-s electron-magnon scattering having a T^2 dependence at low temperatures below 20 K. White

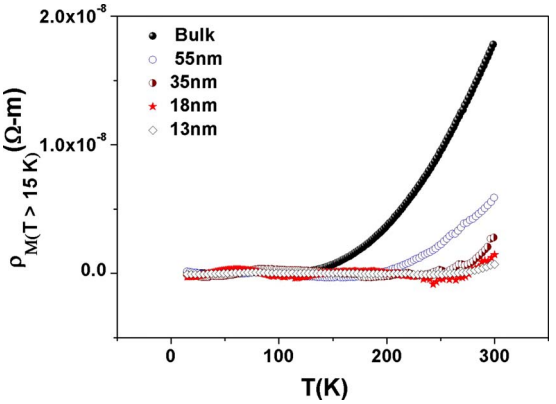

FIG. 9. (Color online) Plot of magnetic part of resistivity $\rho_M(T > 15$ K) versus T for $T > 15$ K.

and Woods[13] experimentally found this behavior in Ni, Fe and Co for temperatures below 10 K. In addition to these reports, Kondorsky *et al.*[24] found that the T^2 behavior continued up to 30 K in these metals. However, Goodings[21] reported that, above 20 K, the electron-magnon scatterings involving the *s-d* transition start dominating the single band *s-s* electron-magnon scattering by an order larger in magnitude. Hence, for better analysis, it is important to include maximum data, but restricting the upper range of temperature to a temperature such as 15 K (as we took in our case) well below 20 K. Second, in our extensive data analysis (both for spin wave and phonon scatterings), 15 K proved to be the optimum temperature for better fits on maximum data with minimum error and best match with previous reports (in case of bulk nickel wire). For $T > 15$ K, the dominance in phonon contribution can be easily understood by the fact that the temperature dependent part was successfully fit by the Bloch-Wilson[11] formula with errors less than 0.4%. It is further evident from Fig. 9 that the phonon contribution is dominant between 15–100 K as the magnetic resistivity starts becoming significant as one reaches temperatures closer to 130 K (in case of bulk wire) and above 180 K (in case of nanowires).

The Debye temperature (θ_D) of a solid as determined from the heat capacity is determined mainly by the sound velocity and, hence, the elastic modulus. An enhancement of the modulus will enhance the sound velocity and hence θ_D. Similar consideration applies to the Debye temperature determined from the resistivity (θ_R). In Fig. 10(a) we collect the data on Ni determined in this investigation as well as the data obtained by our group on two other fcc metals, Cu and Ag. The data are plotted as the ratio $[\theta_R(d)/\theta_R(\text{Bulk})]$ where the symbols in parenthesis refer to the diameter d and the bulk solid respectively. It can be seen that in all the three solids the ratio decreases as d is reduced. (For the two Ag nanowires of smallest diameter, the wires were not fcc but had presence of hcp phase as well.) The results show that the reduction in $\theta_R(d)$ would indicate that the elastic modulus decreases on reduction in d. The fact that in all the three fcc solids, similar behavior is observed establishes that the diameter dependence is robust. Previous experimental studies, those which addressed the issue of size dependence of modulus or the Debye temperature, were done using nanoindentation or by looking at force displacement relation using contact mode atomic force microscopy (AFM). In terms of dependence of elastic modulus on size in these materials, experimental studies offer no convergence. For instance in hydrothermally synthesized Ag nanowires[25] (crystallinity not checked), the elastic modulus increased on size reduction as determined by AFM. For very thin films of Ni (Ref. 26) and Cr (Ref. 27) the modulus as determined by AFM were found to decrease on size reduction. Determination of Young's modulus in Ag (Ref. 28) and Au (Ref. 29) nanowires showed no clear trend as the error bars were large. In many of these experiments the nanowires were polycrystalline or their state of crystallinity were not determined. Interestingly in a very early[30] determination of heat capacity of lead nanoparticles, there was observation of enhancement of the T^3 term and hence lowering of θ_D. We note that in ultrathin Au films grown epitaxially (thickness of 2–70 nm),[31] the Debye temperature (θ_R) was evaluated from the ρ vs T curve using BG theory and θ_R decreased as the diameter (d) was reduced. In the present investigation the use of resistivity to find and investigate the Debye temperature of metallic nanowires is, thus, a fresh approach and it allows higher precision. The nanowires used here also were well characterized and were single crystalline in nature.

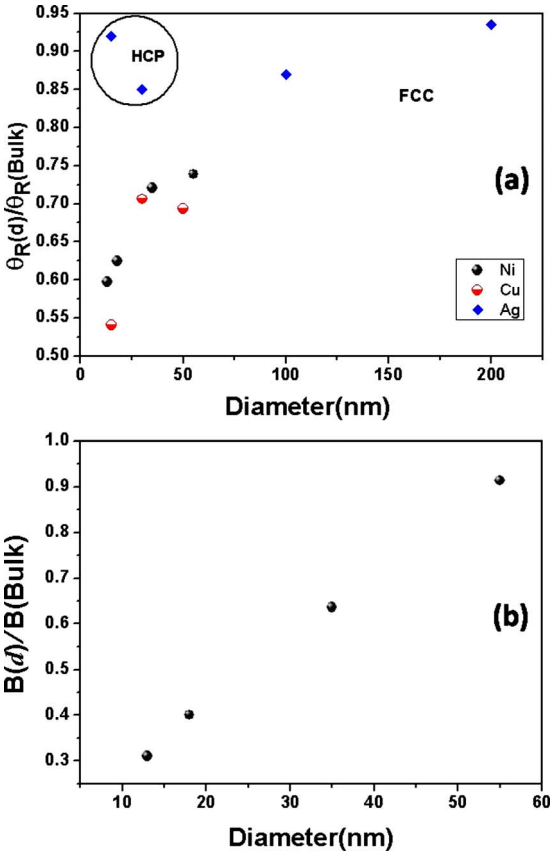

FIG. 10. (Color online) (a) Normalized value of Debye temperature ($\frac{\Theta_R(d)}{\Theta_R(\text{Bulk})}$) of Ni, Cu and Ag nanowires as a function of the wire diameter, (b) Normalized value of magnetic resistivity constant B ($\frac{B(d)}{B(\text{Bulk})}$) as a function of the wire diameter d.

The theoretical reasons for lowering of the modulus of elasticity has been attributed to different types of surface contributions.[32,33] For example, using bond-order-length-strength correlation mechanism, it was shown that Young's modulus as a function of size will reduce or increase as the size is reduced depending on the temperature as well as the change in bond energy in the surface.[32] Using the parameters for metal nanowires, it can be shown that the weakening of surface energy and the enhanced contribution of surface bonds on smaller diameter sample are expected to reduce the elasticity modulus on size reduction at low temperatures. Similar results were also obtained from cohesive energy calculations.[33] These theoretical predictions agree very well with our observation of reduction in θ_R in fcc metal nanowires.

The observation of decrease in B by a large factor when the size is reduced can arise mainly from two factors: (a) a reduction in the *s-d* interaction $NJ(0)$ and (b) a reduction in the magnon effective mass μ. The last alternative seems to

be less likely because the spring stiffness constant $D \propto \mu^{-1}$. This implies that size reduction leads to enhancement of D. However, in a ferromagnet, $T_c \sim D$. Thus, an enhancement of D on size reduction looks unlikely because experimentally we find that size reduction actually leads to a reduction in T_C. It thus appears that our experiment suggests that $NJ(0)$ is reduced on size reduction. We suggest this as a likely mechanism. In nanowires, the contribution of the spins at the surface becomes increasingly important as the size is reduced. These spins sitting in a disordered environment near or at the surface may not support long wavelength propagating spin waves that are needed for the temperature dependent resistivity of the type that gives ρ_M. Instead, they may be overdamped spin waves which will not make any contribution to the spin wave scattering. This will reduce N effectively and will reduce $NJ(0)$. Since $NJ(0)$ appears as a quadratic term, a small decrease can lead to a relatively larger effect in B. (The damped surface spin waves, however, can lead to a static temperature independent scattering. The fact that we see very large diffused electron scattering from the surface leading to low specularity factor p may suggest that this is indeed the case.)

In summary, we have synthesized nickel nanowires within anodic alumina membranes with pore diameter varying from 55 to 13 nm. Resistance measurements were carried out in the temperature range of 3–300 K. The resistance data between 15–100 K has been analyzed using Bloch-Wilson function. The values of Debye temperatures obtained for nanowires decrease with a decrease in the wire diameter which we consistently find for other fcc metal nanowires. However, we find the electron-phonon coupling constant is nearly unchanged on size reduction down to 13 nm. The experiment allowed us to determine the absolute value of the residual resistivity (at 4.2 K). Using the Dingle and Sondheimer theories, we analyzed the data and found that the surface scattering plays a major role in the high resistivity values in case of nanowires. The electron mean free path is limited mainly by the diffused surface scattering and the highly crystalline nature of the wire ensures that there are negligible scattering of electrons by defects within the bulk of the wires. The data for temperature $T < 15$ K can be analyzed including the magnetic scattering term and we observed a large change as one goes down to the nanoscale. Even for temperature $T > 15$ K, we observed a decrease in the magnetic contribution. Thus, over the whole temperature range we observed a suppression in the magnetic contribution to the resistivity as we lower the wire diameter.

ACKNOWLEDGMENTS

The authors thank the Unit of NanoScience, IACS, Kolkata for TEM support. This work is financially supported by the Department of Science and Technology, Government of India and CSIR, Government of India.

*venkat@bose.res.in
†arup@bose.res.in

[1] L. Sun, P. C. Searson, and C. L. Chien, Phys. Rev. B **61**, R6463 (2000).
[2] R. Ferré, K. Ounadjela, J. M. George, L. Piraux, and S. Dubois, Phys. Rev. B **56**, 14066 (1997).
[3] W. Wernsdorfer, K. Hasselbach, A. Benoit, B. Barbara, B. Doudin, J. Meier, J.-Ph. Ansermet, and D. Mailly, Phys. Rev. B **55**, 11552 (1997).
[4] C. Durkan and M. E. Welland, Phys. Rev. B **61**, 14215 (2000).
[5] W. Steinhogl, G. Schindler, G. Steinlesberger, and M. Engelhardt, Phys. Rev. B **66**, 075414 (2002).
[6] W. Steinhogl, G. Schindler, G. Steinlesberger, M. Traving, and M. Engelhardt, Phys. Rev. B **66**, 075414 (2002).
[7] W. Wu, S. H. Brongersma, M. Van Hove, and K. Maex, Appl. Phys. Lett. **84**, 2838 (2004).
[8] D. Josell, C. Burkhard, Y. Li, Y. W. Cheng, R. R. Keller, C. A. Witt, D. R. Kelley, J. E. Bonevich, B. C. Baker, and T. P. Moffat, J. Appl. Phys. **96**, 759 (2004).
[9] A. Bid, A. Bora, and A. K. Raychaudhuri, Phys. Rev. B **74**, 035426 (2006).
[10] J. M. Ziman, *Electrons and Phonons* (Clarendon, Oxford, 1960).
[11] H. Wilson, Proc. R. Soc. London, Ser. A **167**, 580 (1938).
[12] I. Mannari, Prog. Theor. Phys. **22**, 335 (1959).
[13] G. K. White and S. B. Woods, Philos. Trans. R. Soc. London, Ser. A **251**, 273 (1959).
[14] URL: http://www.synkera.com/
[15] Cryomech, Model PT405 Cryogenic Refrigerator, 113 Falso Drive, Syracuse, New York 13211, USA.
[16] A. Bid, A. Bora, and A. K. Raychaudhuri, Nanotechnology **17**, 152 (2006).
[17] A. Bid, A. Bora, and A. K. Raychaudhuri, Phys. Rev. B **72**, 113415 (2005).
[18] M. N. Ou, T. J. Yang, S. R. Hartyunyan, Y. Y. Chen, C. D. Chen, and S. J. Lai, Appl. Phys. Lett. **92**, 063101 (2008).
[19] R. B. Dingle, Proc. R. Soc. London, Ser. A **201**, 545 (1950).
[20] E. H. Sondheimer, Adv. Phys. **1**, 1 (1952).
[21] D. A. Goodings, Phys. Rev. **132**, 542 (1963).
[22] T. Kasuya, Prog. Theor. Phys. **16**, 58 (1956).
[23] E. A. Turov, Izv. Akad. Nauk SSSR, Ser. Fiz. **19**, 426 (1955).
[24] E. Kondorsky, O. S. Galkina, and L. A. Tchernikova, J. Appl. Phys. **29**, 243 (1958).
[25] G. Y. Jing, H. L. Duan, X. M. Sun, Z. S. Zhang, J. Xu, Y. D. Li, J. X. Wang, and D. P. Yu, Phys. Rev. B **73**, 235409 (2006).
[26] M. Kopycinska-Muller, R. H. Geiss, J. Muller, and D. C. Hurley, Nanotechnology **16**, 703 (2005).
[27] S. G. Nilsson, X. Borrise, and L. Montelius, Appl. Phys. Lett. **85**, 3555 (2004).
[28] B. Wu, A. Heidelberg, J. J. Boland, J. E. Sader, X. Sun, and Y. Li, Nano Lett. **6**, 468 (2006).
[29] B. Wu, A. Heidelberg, and J. J. Boland, Nature Mater. **4**, 525 (2005).
[30] V. Novotny, P. P. M. Meincke, and J. H. P. Watson, Phys. Rev. Lett. **28**, 901 (1972).
[31] G. Kastle, H. G. Boyen, A. Schroder, A. Plettl, and P. Ziemann, Phys. Rev. B **70**, 165414 (2004).
[32] M. X. Gu, C. Q. Sun, Z. Chen, T. C. Au Yeung, S. Li, C. M. Tan, and V. Nosik, Phys. Rev. B **75**, 125403 (2007).
[33] C. C. Yang and S. Li, Phys. Rev. B **75**, 165413 (2007).